Chemical Physics Letters 556 (2013) 230–236

Contents lists available at SciVerse ScienceDirect

Chemical Physics Letters

journal homepage: www.elsevier.com/locate/cplett

Noncovalent interaction and its influence on excited-state behavior: A theoretical study on the mixed coaggregates of dicyanonaphthalene and pyrazoline

Yulan Dai [a], Meiyuan Guo [a], Jingdong Peng [a,*], Wei Shen [a], Ming Li [a,b], Rongxing He [a,b,*], Chaoyuan Zhu [c], Sheng Hsien Lin [c]

[a] School of Chemistry and Chemical Engineering, Southwest University, Chongqing 400715, China
[b] Education Ministry Key Laboratory on Luminescence and Real-Time Analysis, Southwest University, Chongqing 400715, China
[c] Department of Applied Chemistry, Institute of Molecular Science and Center for Interdisciplinary Molecular Science, National Chiao-Tung University, Hsinchu 300, Taiwan

ARTICLE INFO

Article history:
Received 9 October 2012
In final form 22 November 2012
Available online 3 December 2012

ABSTRACT

In the present letter we investigate the noncovalent interactions in the mixed coaggregates of 1,3,5-triphenyl-2-pyrazoline (TPP) and 1,4-dicyanonaphthalene (DCN) and their influence on the excited-state properties of the TPP–DCN. The theoretical results show that the π–π stacking interactions play an important role in the noncovalent interactions of the TPP–DCN coaggregates. The effect of the π–π interactions on the excited-state properties of the TPP–DCN is also fully investigated, and the results indicate that the TPP and DCN do not form an intermolecular charge-transfer complex in the ground state, whereas they form an exciplex in the excited state.

1. Introduction

Noncovalent interactions play a crucial role in many areas of chemistry, biology, and materials science [1–3]. As one of the principal nocovalent interactions, the π–π stacking is essential to understand and explain many supramolecular organization and recognition processes [4,5], such as nucleic acids [6,7], porphyrin-like aggregates [8] and macromolecular structures [9,10]. Because of their importance for the design of novel supramolecular systems and nanomaterials, the π–π stacking interactions have been studied extensively in the past decades . In order to understand the nature of the π–π stacking interactions, the benzene dimer was investigated experimentally and theoretically as one of the simplest prototypes of π–π stacking interactions [11–15]. Theoretical computations indicated that the displace-stacked and T-shaped (edge-to-face) structures of the benzene dimer are the most stable ones because of the quadrupole–quadrupole interactions. However, only the T-shaped configuration was observed experimentally [11]. For the substituted benzene dimer, the situation is different from that of the benzene dimer due to the inductive effect of substituent group which alters energy landscape [16]. In some cases of given systems, the stacked configurations are predicted to be more stable than the T-shaped one because the dipole–dipole attractive interactions overwhelm the quadrupole–quadrupole repulsive interactions. Actually, the nature of the π–π stacking interactions is still a matter of debate [17,18]. Hobza et al. [2,3,19] and Improta et al. [20–22] performed a series of theoretical studies to explore the nature of noncovalent interactions and to explain their influence on the ground and excited states of given systems, such as nucleic acids and dye aggregates. They studied the electronic state, decay rate and quantum dynamics of nucleic acids using the intermolecular charge transfer (CT) character in the density functional theory (DFT) framework. These theoretical works provided a step forward to understand the nature of noncovalent interactions and photoinduced charge transfer (PCT) process. In general, the interaction energies between two molecules include the electrostatic interactions, induction interactions, dispersion interactions and repulsive interactions. The central issue is to make clear the extent of these components contributing to final interaction enthalpy in the ground state. For the excited state, ones focus their efforts to the influence of weak interactions on ionization energies, decay rate and quantum dynamics.

The calculation of intermolecular energies is one of the difficult tasks in today's computational chemistry [23]. To describe exactly the intermolecular energies, many theoretical efforts have been performed [24–31]. Highly accurate coupled cluster methods (CCSD(T)) are available for small molecular systems [27]. For supermolecule, however, this methodology is not appropriate because of the expensive computational cost, which makes people to use more suitable methods, such as the DFT method. Unfortunately, the traditional DFT (such as B3LYP) methods generally show a dramatic underestimation of the weak interactions for noncovalent systems. In the last decade, scientists have developed a series of new DFT methods including the dispersion correction

* Corresponding authors at: School of Chemistry and Chemical Engineering, Southwest University, Chongqing 400715, China. Fax: +86 23 68254000 (R. He).
E-mail addresses: hxpengjd@swu.edu.cn (J. Peng), herx@swu.edu.cn (R. He).

0009-2614/$ - see front matter © 2012 Elsevier B.V. All rights reserved.
http://dx.doi.org/10.1016/j.cplett.2012.11.061

term, such as the M0X (X = 5, 6) family [28], the dispersion-correcting atom-centered potentials (B3LYP-DCPs) [29] and the Grimme's DFT-D [30] method. These methods have an outstanding performance to describe the π–π stacking interactions, especially the ωB97XD functional of Grimme's DFT-D [31] method.

The PCT process is a primary step in photophysical, photochemical as well as photobiological processes. The PCT process can be intermolecular CT in which an electron is transferred from donor to acceptor. In earlier PCT studies, the covalent linked and hydrogen-bonded donor–acceptor self-assembled aggregates were investigated mainly. Since the PCT process in coaggregates (one of kinds of aggregates) was found occasionally by Janssen and co-workers [32], the research of coaggregates has made great progress, especially in the area of supramolecular engineering of functional dyes. The most attractive features of dye aggregates are their emerging new functionalities which are not given in individual molecule but arisen upon in aggregation due to the electronic coupling of π-systems [33]. These functionalities render dye aggregates have the possibilities of application in novel technological areas, such as nanomaterials, organic semiconductors and solar cells [32–35].

Yao et al. [36] studied the PCT process of the mixed coaggregates TPP–DCN containing 1,3,5-triphenyl-2-pyrazoline (TPP) and 1,4-dicyanonaphthalene (DCN) both in experiment and theory. In the TPP–DCN, the TPP group acts as an electron donor and the DCN moiety is used as an electron acceptor. As reported in Ref. [36], for the ground state of the TPP–DCN, the pyrazoline ring of the TPP and the naphthalene ring of the DCN are in a face-to-face stacking mode. Through analyzing the properties of experimental spectra, they considered that the π–π stacking has effect on the electron transfer process, and an intermolecular charge-transfer complex between the TPP and DCN groups should be formed in the excited state but not in the ground state (S_0). Recently, Chen and his co-workers [37] investigated the PCT process and excited-state properties of the TPP–DCN using the TDDFT method. They concluded that the PCT mechanism for the TPP–DCN was the mixture of intermolecular and intramolecular CT in the vertical absorption process. The phenyl group of the TPP monomer plays a role of electronic donor both in intramolecular and intermolecular CT processes. These studies provided a well explanation for the CT processes of the TPP–DCN. However, the nature of the π–π stacking interactions in the TPP–DCN is important to understand the PCT mechanism [37]. To our best knowledge, the theoretical studies on the π–π stacking interactions of the TPP–DCN coaggregates and their influence on the excited-state properties are still not reported. Moreover, the B3LYP functional is not suitable to describe the π–π stacking interactions, because it is defective in the description of the dispersion interactions [2].

To further understand the PCT process, in the present letter we investigated the nature of the π–π stacking interactions and their influence on the excited-state behavior of the TPP–DCN coaggregates. As mentioned above, in this letter the ground- and excited-state geometries of the TPP–DCN are optimized with the new DFT methods, such as the ωB97XD functional. Then the spectral properties, charge-transfer character and π–π stacking interactions of the TPP–DCN are investigated in detail based on the optimized geometries.

2. Computational details

All calculations are performed with the GAUSSIAN 09 program [38]. The monomer geometries optimized at the B3LYP/6-311++G(d,p) level are used to construct the stacking mode of the TPP–DCN. In order to ensure the optimized geometries of the TPP–DCN are reasonable, the traditional (B3LYP and PBE0) and new (ωB97XD, M06-2X and B3LYP-DCP) functionals are used and their results are compared with each other and with the previous theoretical data. It is notable that the traditional functionals give the displace-stacked and T-shaped structures of the TPP–DCN, while the new functionals only provide the displace-stacked configuration. Considering the outstanding performance of the new functional to describe the π–π stacking interactions and our main purpose, only the displace-stacked configuration is discussed in the present letter. Frequency calculations at the same levels are performed to confirm each stationary point to be a true energy minimum. According to the results of potential energy curves (PECs) (Fig. S1 and Table S1), the new functionals do provide well-defined minima of the TPP–DCN with the equilibrium distances 3.6–3.7 Å between the TPP and DCN. Based on the optimized geometries, the TDDFT with the 6-311++G(d,p) basis set is used to predict vertical excitation energies (VEE). The excited-state structure of the TPP–DCN is optimized using the smaller basis set (6-31G(d)) due to the expensive computational cost of the excited-state frequency calculation. Solvent effects on the geometries and on the excited-state properties have also been included by using the Polarizable Continuum Model (PCM) [39] (in water). As is well known [36], the planarity and hydrophobic property can encourage the formation of π–π stacking in polar solvents.

The Multiwfn 2.3 program [40] is used to perform the charge transfer analysis. In addition, this code can provide information about the characteristic of π–π stacking interactions and molecular orbital (MO) compositions. A graphical representation of characteristic is displayed using the VMD 1.9 [41] and Molekel programs [42]. The Huang–Rhys (HR) factors are calculated based on the optimized geometries and the vibration-normal-mode frequencies of the ground and the first excited states with our own code.

3. Results and discussion

3.1. Geometry structures of the coaggregates

The optimized geometries of the monomers and the TPP–DCN coaggregates are shown in Figure 1. Their ground-state structures are calculated at the ωB97XD/6-311++G(d,p) level, while the excited-state geometry of the TPP–DCN is optimized at the ωB97XD/6-31G(d) level. Some important structural parameters characterizing relative difference between the monomers and stacked complex are defined and listed in Table 1. In the DCN, the dihedral angle D1 (N16–C15–C14–13) and D2 (N12–C11–C10–C9) are both almost 180°, while in the TPP–DCN they are about 89.04° and −75.63°, respectively. This indicates that the distortion of DCN in the TPP–DCN is due to the steric hindrance and electrostatic repulsion. In the TPP, the dihedral angle D3 (C1–N2–N3–C4) is defined to describe the coplanarity of pyrazoline ring. The calculations show that the change of D3 is small when the TPP–DCN is formed (the value is 9.36° and 7.16° in the TPP–DCN and the TPP monomer, respectively). Obviously, the neglectable change of D3 indicates an excellent coplanarity of pyrazoline ring, which is favorable to form the TPP–DCN stacking system due to the π–π stacking interactions between the TPP and DCN. In the TPP–DCN, the stacking distance d1 between the TPP and DCN calculated at the ωB97XD/6-311++G(d,p) level is about 3.34 Å (the B3LYP distance is 3.9 Å [36]). The accurate description of the stacking distance is beneficial to understand the influence of the π–π interactions on the electron transfer mechanism. We believe that the present results are more reasonable than the previous theoretical calculations because the ωB97XD functional includes the dispersion correction term.

According to the optimized geometries, several important changes going from the S_0 to the first excited state (S_1) should be noted. The dihedral angle D6 (N2–N3–C9–C10) describing the

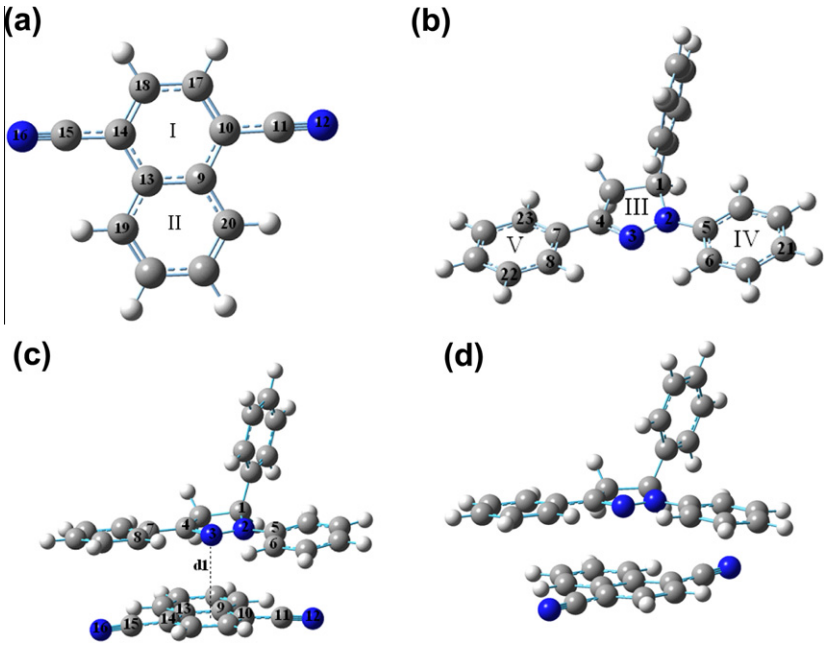

Figure 1. Optimized structures of the monomers and coaggregates. (a) DCN; (b) TPP; (c) ground state and (d) excited state of the TPP–DCN coaggregates. The vertical distance between TPP and DCN is described as d1. The geometry of ground state of the mixed coaggregates is optimized at the ωB97XD/6-311++G(d,p) level and that of the excited state is obtained at ωB97XD/6-31G(d) level.

Table 1
Selected geometrical parameters of monomers and the TPP–DCN coaggregates calculated by the ωB97XD theoretical level. The atom numbering is showed in Figure 1.

Parameters	TPP[a]	DCN[a]	TPP–DCN(S_0)[a]	TPP–DCN(S_1)[b]
D1(N16-C15-C14-C13)		180	89.04	92.30
D2(N12-C11-C10-C9)		180	−75.63	58.21
D3(C1-N2-N3-C4)	7.16		9.36	4.42
D4(N3-N2-C5-C6)	0.87		7.53	−3.07
D5(N3-C4-C7-C8)	5.49		8.83	3.56
D6(N2-N3-C9-C10)			78.18	48.80
d1			3.34	3.28

[a] Calculated by the ωB97XD/6-311++G(d,p) theoretical level.
[b] Calculated by the ωB97XD/6-31G(d) theoretical level.

relative location of the TPP and DCN, has the largest change by comparing the S_0 and S_1. As shown in Table 1, D6 is about 78.18° in the S_0 state, while it is only 48.80° in the S_1 state. In addition, the distortion of the DCN is very large as displayed by the change of D1 and D2 (they are 89.04° and −75.63° for S_0 state, 92.30° and 58.21° for S_1 state). These suggest that the Huang–Rhys factors should be very large. However, the planarity of the pyrazoline ring is still retained very well (D3 changes from 9.36° to 4.42°), which is important to form the π–π stacking TPP–DCN coaggregates regardless of the S_0 and S_1 states. Further, we find that the change of the distance d1 is also very small (changes from 3.34 Å of the S_0 to 3.28 Å of the S_1). Besides, to check how the solvent effect on the geometries, we also optimize the TPP–DCN structure in gas phase. The change trend of the stacking structures in vacuum is similar to those in solution (see Table S2 in SI). These changes of geometries of the S_0 and S_1 states can enhance our understanding of the stacking effects on the excited-state properties of the TPP–DCN.

3.2. The noncovalent interactions in the coaggregates

A visualization analysis of the noncovalent interactions is made to understand the nature of nonbonded interactions in the TPP–DCN coaggregates. Yang and his co-workers [43] developed an approach to detect the noncovalent interactions in real space, based on the electron density (ρ) and its derivatives. In the present letter we utilize this approach to identify the type of the nonbonded interactions in the TPP–DCN, which is important to reveal the nature of the analogous mixed coaggregates. Our calculated results are shown in Figure 2A, in which the vertical coordinate represents the reduced density gradient (RDG), and the horizontal coordinate is sign(λ_2). RDG is a fundamental dimensionless quantity coming from the density and its first derivative ($RDG = 1/(2*(3*\pi^{\wedge}2)^{\wedge}(1/3))|\nabla\rho(\gamma)|/\rho^{\wedge}(4/3)$, and sign(λ_2) is defined as a physical quantity that the electron density multiplies by the sign of the second Hessian eigenvalue λ_2. For the details that how to distinguish different types of noncovalent interactions, ones are encouraged to recourse the Ref. [43].

As shown in Figure 2A, we find that two low-density, low-gradient spikes are very close to zero in the plot of RDG vs. sign(λ_2) ρ for the TPP–DCN coaggregates. According to the conclusions presented in Ref. [43], the low-density, low-gradient spike with slightly negative value indicates weak attractive interactions (>−0.010 a.u.). Conversely, the low-density, low-gradient spike remains at a slightly positive value indicates a weak repulsion interactions (<0.010 a.u.). For the first case, the weak attraction interactions should be the key factor to form the TPP–DCN. As we know that the intermolecular weak interactions include the hydrogen bonds, stacking interactions, electrostatic interactions and hydrophobic interactions [2]. Therefore, we are very curious to know which force will be dominant to form the TPP–DCN coaggregates. Considering the geometries of the monomers of TPP and DCN, we can easily find that both of them have aromatic structures with conjugated π electrons. This implies the π–π stacking effect should be strong when the TPP closes to the DCN in a parallel manner. In other words, the main composition of noncovalent interactions in the TPP–DCN should be the π–π stacking interactions. The plot of RDG vs. sign(λ_2) provides a rich visualization of this weak π–π attraction, which is showed as a spike at the bottom-left point in Figure 2A where sign(λ_2) is about −0.002 a.u. To confirm the validity about the nature of noncovalent interactions, we calculate the low-gradient (RDG = 0.6 a.u.) isosurfaces which subjects to the constraint of low density for the TPP–DCN, and the result is

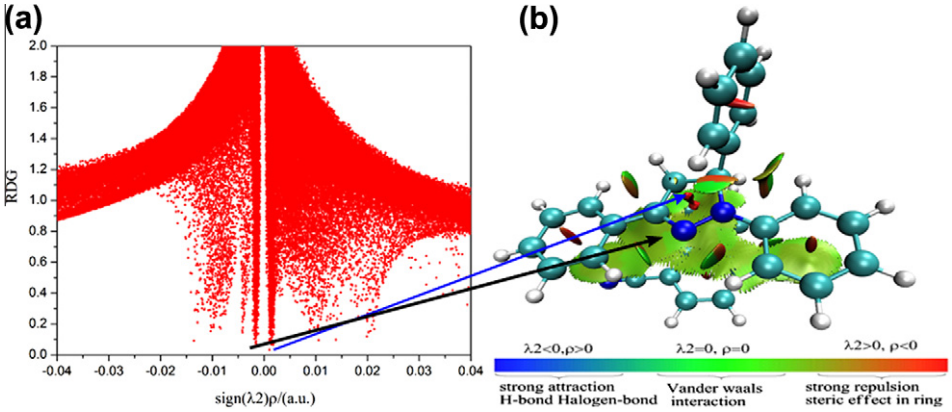

Figure 2. The π–π stacking interactions in TPP–DCN mixed aggregates. Plots of the reduced density gradient vs. the electron density multiplied by the sign of the second hessian eigenvalue.

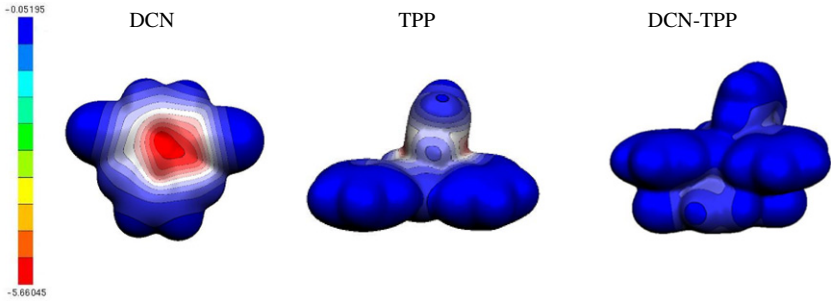

Figure 3. Electrostatic potential maps of the monomers TPP and DCN, TPP–DCN calculated at the ωB97XD/6-311++G (d,p) level in aqueous solution.

displayed in Figure 2B. In the plot of low-gradient isosurfaces, a density cutoff of $\rho < 0.05$ a.u. is chosen since it encapsulates the interesting noncovalent interactions region (see Figure 2A). Obviously, in the TPP–DCN, there is an area of nonbonded overlap located at the whole molecular planes of the TPP and DCN moieties, particularly at the centers of ring III (pyrazoline) of the TPP and ring I (benzene) of the DCN. This area of low-gradient isosurface is colored as green[1] (links the spike at the bottom-left point in Figure 2A by using black arrow) according to the corresponding values of sign(λ_2)ρ. The π–π stacking interactions are manifested by the isosurface filling the space between the molecular planes of the TPP and DCN groups. For the second case, the weak repulsion interactions (as shown by the spike at the bottom-right point in Figure 2A where sign(λ_2)ρ is about 0.002 a.u.) between the TPP and DCN also can be pictured by the same method. When the TPP gradually closes to the DCN, the repulsion force will become larger until it finally equals to the π–π attraction force. We consider that this equilibrium leads to the formation of the stable TPP–DCN coaggregates. In addition, almost no blue or even cyan isosurfaces can be observed, indicating that the dimeric stablization is dominated by π–π stacking interactions rather than hydrogen bonds. Noted that the red isosurfaces at the centers of molecular rings denote the steric repulsion, which is linked to the plot of RDG vs. sign(λ_2)ρ with a blue arrow.

Let us now analyze the results related to the π–π stacking interactions in the TPP–DCN coaggregates. In this letter the electrostatic potential surfaces of the TPP, DCN and TPP–DCN are also calculated, and the maps are shown in Figure 3. The red areas indicate more negative electron density, while blue areas denote more positive electron density. Inspection of the maps shows that the negative charge is centered on the ring I of the DCN and the ring VI of the TPP, while the positive charge is concentrated on the side of the DCN and the ring III of the TPP. Apparently, the electrostatic attraction mainly take place between the ring I of the DCN and ring III of the TPP. As a composition of the π–π stacking interactions, the electrostatic interactions play an important role in the formation of the π–π stacking TPP–DCN coaggregates.

3.3. The absorption features of the coaggregates

As mentioned in Introduction, Yao et al. [36] considered that an intermolecular charge-transfer complex between the TPP and DCN moieties should be formed in the excited state but not in the ground state. To inspect the influence of π–π stacking on spectral properties, we calculate the absorption and emission spectra of the TPP–DCN with the traditional and new DFT methods. The results of these methods are almost consistent with each other although the obtained transition order from them is slightly different. For example, the most intense transitions are the second (S_2) and the third excited (S_3) states for new DFT methods, but they are S_3 and S_4 (the fourth excited state) states for the traditional DFT methods. Therefore, in the following only the ωB97XD results are discussed.

The calculated UV–vis absorption spectra of the TPP–DCN, pure TPP and DCN monomers in water are shown in Figure 4a. As listed in Table 2, the theoretical absorption peak of the TPP is about 322.81 nm, the peaks of the DCN appear at 308.08 and 222.92 nm, and the bands of the TPP–DCN locate at 328.29 and 223.87 nm. These results agree well with the experimental [36] and previous theoretical counterparts [36,37], indicate that the optimized geometries of these compounds are reasonable and

[1] For interpretation of color in Figure 3, the reader is referred to the web version of this article.

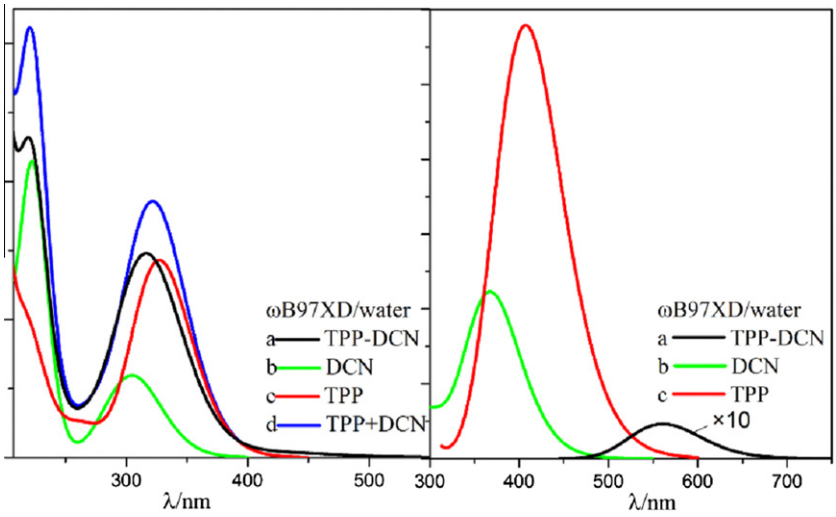

Figure 4. Calculated absorption and emission spectra using the ωB97XD functional. (a) The absorption spectra calculated at the ωB97XD/6-311++G(d,p) level. (b) The emission spectra calculated at the ωB97XD/6-31G(d) level.

Table 2
Computed vertical excitation energies of monomers and the TPP–DCN coaggregates using different theoretical levels.

	Energy (osc.str.)	Orbitals[a]
TPP		
ωB97XD/6-311++G(d,p)		
S_1	322.81(0.5981)\365[b]	H → L
S_2	283.02(0.0677)	H → L + 1
S_3	222.92(0.8142)	H → L + 2
S_4	222.56(0.2284)	H-5 → L; H → L + 3
DCN		
ωB97XD/6-311++G(d,p)		
S_1	308.08(0.2603)321[b]	H → L
S_2	299.31(0.0632)	H-1 → L; H → L + 1
S_3	289.96(0.0108)	H-2 → L + 1 ;H-1 → L; H → L + 1; H-1 → L + 2
S_4	283.59(0.0302)	H-2 → L
TPP–DCN		
ωB97XD/6-311++G(d,p)		
S_1	418.77(0.0102)	H → L
S_2	328.29(0.3764)	H-1 → L; H → L + 1; H → L + 2
S_3	305.38(0.4189)	H-1 → L; H → L + 1
S_4	282.22(0.0395)	mixed → L; mixed → L + 2
PBE0/6-311++G(d,p)		
S_1	621.69(0.0003)	H → L
S_2	373.93(0.4583)	H → L + 1
S_3	346.22(0.0028)	H → L + 2
S_4	337.25(0.2404)	H-1 → L; H-10 → L
M062X/6-311++G(d,p)		
S_1	433.24(0.0105)	H → L
S_2	332.30(0.3773)	H → L + 1;H-1 → L;H → L + 2
S_3	303.16(0.3692)	H → L + 1;H-1 → L;H-2 → L
S_4	289.66(0.0275)	H → L + 1; H → L + 2
B3LYP/6-31G[b,c]		
S_1	647.24(0.0011)	H → L
S_2	368.62(0.4502)	H → L + 1;H-1 → L
S_3	344.14(0.0017)	H → L + 2;H-1 → L
S_4	341.45(0.2019)	H → L + 1;H → L + 2;mixed → L
B3LYP/6-31+G(d,p)-DCP		
S_1	636.27(0.0184)	H → L
S_2	384.86(0.1124)	H-1 → L; H → L + 1; H → L + 2
S_3	361.81(0.1148)	H-1 → L; H → L + 1; H → L + 2
S_4	349.81 (0.0406)	H-2 → L; H-1 → L; H → L + 1

[a] Assignment: H = HOMO, L = LUMO, L − 1 = LUMO-1, H-1 = HOMO-1, etc.
[b] Ref. [36].
[c] Ref. [37].

the selected method is reliable. Further, we find that the spectrum of the TPP–DCN is almost identical to the linear superposition of the spectra of the pure DCN and TPP monomers, and the singlet excited-state energy level of the TPP (3.99 eV) lies below that of the DCN (4.06 eV). These imply that the TPP and DCN do not form an intermolecular charge-transfer complex in the mixed coaggregates. That is, the present calculations approve the experimental consequence that the π–π stacking interactions has no remarkable influence on the absorption spectrum of the ground state of the TPP–DCN (thus an intermolecular charge-transfer complex in ground state of the mixed coaggregates is not formed).

However, does an intermolecular charge-transfer exciplex (excited-state complex) can be generated? Most importantly, how to explain the experimental results? These are very important to help ones understand the nature of PCT, which could provide insights for understanding other analogous systems. In the present letter we use the absorption spectra, emission spectra and frontier molecular orbital theory to investigate the intermolecular charge-transfer of excited state, and the theoretical results can satisfactorily explain the experimental details [36].

For the TPP–DCN, the calculated oscillator strengths of vertical excitation from the ground state to excited states are reported in Table 2. To obtain a sufficiently large pool of excited states for the relevant excitations, we calculate the first 10 vertical excitation energies, and only four main excited states with large oscillator strengths are given in Table 2. The relative strengths are 0.0102, 0.3764, 0.4189 and 0.0395 for the excitations $S_0 \rightarrow S_1$, $S_0 \rightarrow S_2$, $S_0 \rightarrow S_3$ and $S_0 \rightarrow S_4$, respectively. The S_1 is resulted mainly from the electron excitation from the highest occupied orbital HOMO to the lowest unoccupied orbital LUMO. According to the results of the molecular orbital fragment analyses (Figure 5), HOMO is composed of 99.6% HOFO (HOMO of fragment orbital) of the TPP fragment, and LUMO is nearly formed by 98.6% LUFO (LUMO of fragment orbital) of the DCN moiety. That is, HOMO and LUMO of the TPP–DCN are π-type orbitals mainly located at the DCN and TPP moieties, indicating that the S_1 is a CT state with transition forbidden characteristic. The two excited states, S_2 and S_3, possess the largest oscillator strengths among the four excited states (see Table 2). The S_2 is contributed mainly from HOMO to LUMO + 1, the S_3 mainly from HOMO-1 → LUMO. As shown in Figure 5, HOMO-1 is a π-type orbital located on the DCN moiety, and LUMO + 1 is also a π-type orbital located on the TPP group. Thus the S_2 and S_3 are local excitation (LE) states.

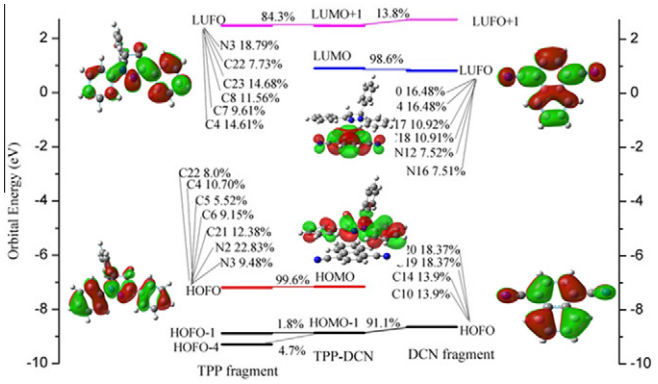

Figure 5. Composition analysis of fragment molecular orbital based on the ωB97XD/6-311++G(d,p) results.

The effect of π–π stacking on the emission spectrum is also examined by the same methods (Figure 4b). The calculated emission peaks of the TPP, DCN and TPP–DCN respectively are 407.32, 367.83 and 560.53 nm (the corresponding experimental data [36] are 456, 396 and 560 nm). Evidently, the origin of the red-shifted emission at about 560 nm is neither from the TPP nor from the DCN. Further, we also calculate the fluorescence spectrum of the TPP–DCN using its S_1 geometry, and the band locates at about 418.77 nm. The present result indicates that the emission band of 560.53 nm does come from a new structure, which is the so-called excited-state complex (exciplex) of the TPP–DCN. As discussed in Subsection 3.1, there is a large change between the geometries of the S_0 and S_1. As we know that the structural difference will result in the redistribution of molecular charge. For the transition of $S_0 \rightarrow S_1$, the transferred charge amount is about 1.34 (see Table S3 in SI) estimated at the ωB97XD/6-311++G(d) level. This implies that the S1 is indeed a CT state due to the π–π stacking effect. In fact, the calculated dipole moment also confirms the result. As displayed in Table S3, the calculated dipole moment of the S_0 is about 5 Debye (D), but that of the S_1 is beyond 17 D. A large change of dipole moment indicates a charge separation in the S_1. Obviously, this result suggests that there are prominent electronic interactions between the TPP and DCN components in the S_1, which indicates that the TPP and DCN in the mixed coaggregates do form an intermolecular charge-transfer complex through direct photoexcitation. Our theoretical discovery agrees well with the experimental conclusion [36].

Is it reasonable that there is a large geometrical change between the S_0 and S_1 states to produce an exciplex (CT state)? To explore this photophysical property, we calculate the Huang–Rhys (HR) factor of every vibrational normal mode of the TPP–DCN. The HR factor reflects the degree of geometrical change along with the vibrational normal coordinates when electron transfers from one state to another state. For the ith mode, the HR factor can be expressed as:

$$S_i = \omega_i d_i^2 / 2\hbar \tag{1}$$

in which ω_i is the harmonic frequency of the ith normal mode, d_i denotes the displacement which can be simply calculated by

$$d_i = Q_i' - Q_i = \sum_j L_{ij}\left(q_j' - q_j\right) \tag{2}$$

where q_j' and q_j are the mass-weighted Cartesian coordinates at the equilibrium geometries of the S_0 and S_1 states, and the transformation matrix L in Eq. (2), along with $q_j'(q_j)$, is calculated by using GAUSSIAN 09 program package. The obtained HR factors are depicted in Figure 6. We can see some of these modes have large HR factors, such as the mode with frequency 1492.99 cm^{-1} has the largest HR factor (260.85). According to Eq. (1), the HR factors are determined

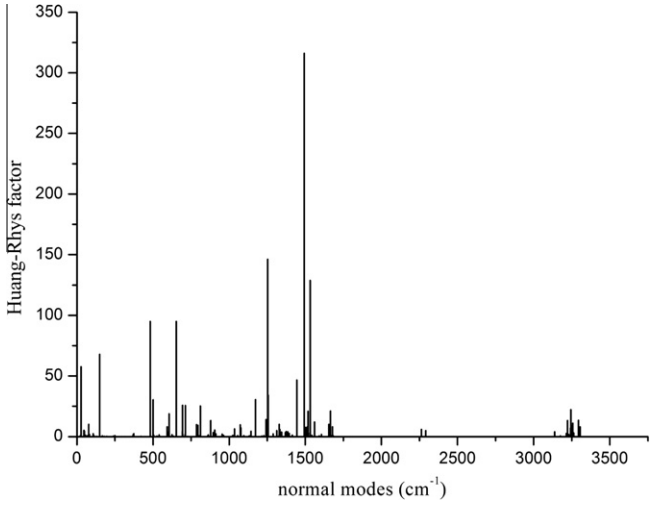

Figure 6. Calculated Huang–Rhys factors vs. normal mode frequencies for the TPP–DCN coaggregates using the ωB97XD/6-31G(d) level.

mainly by the displacement d_i. Thus, the large HR factor indicates a distinct geometrical change between the ground and excited states. Further, we find that the mode with frequency 1492.98 cm^{-1} corresponds to the rotational vibration between the TPP and DCN moieties in the TPP–DCN. This implies that the dihedral angle D6 should change sharply when photoexcitation occurs. Actually, the calculated structural parameters have demonstrated this result (D6 changes from 78.18° (S_0) to 48.80° (S_1)). Therefore, it is reasonable that there is a large geometrical change when electron transitions from the S_0 to S_1, which leads to a charge-separated excited state.

4. Conclusion

In the present letter we optimize the geometries of the S_0 and S_1 states of the TPP–DCN coaggregates, and investigate the nature of the π–π stacking interactions and the influence on the excited-state behavior. Our study indicates that there is a large structural change between the S_0 and S_1 states, which leads to the redistribution of charge in the S_1. This result is proved by the calculated Huang–Rhys factors. Using the approach developed by Yang et al. [43], we detect the noncovalent interactions of the TPP–DCN in real space based on the electron density and its derivatives, and find that the π–π attraction between the TPP and DCN is the main driving force to form the TPP–DCN coaggregates. That is, the π–π stacking interactions play an important role in the nonbonded interactions. In addition, we also examine the influence of the π–π stacking interactions on the excited-state behavior of the TPP–DCN. The calculated results suggest that the TPP and DCN do not form an intermolecular charge-transfer complex in the ground state, whereas they form an exciplex in the excited state. The present theoretical results can satisfactorily explain the experimental details, and are expected to help us understand the nonbonded interactions nature and PET process of other analogous mixed coaggregates.

Acknowledgment

This letter was supported by the National Natural Science Foundation of China (Nos. 20803059 and 21173169).

Appendix A. Supplementary material

Supplementary data associated with this article can be found, in the online version, at http://dx.doi.org/10.1016/j.cplett.2012.11.061.

References

[1] R.A. Kumpf, D.A. Dougherty, Science 261 (1993) 1708.
[2] K. Muller-Dethlefs, P. Hobza, Chem. Rev. 100 (2000) 143.
[3] J. Černý, P. Hobza, Phys. Chem. Chem. Phys. 9 (2007) 5291.
[4] M. Pastore, F.D. Angelis, ACS Nano 4 (2009) 556.
[5] M. Chourasia, G.M. Sastry, G.N. Sastry, Int. J. Biol. Macromol. 48 (2011) 540.
[6] S. Burley, G. Petsko, Science 229 (1985) 23.
[7] C.A. HunterJuswinder, J.M. Thornton, J. Mol. Biol. 218 (1991) 837.
[8] T. Kobayashi, J-aggregates, World Scientific Publishing Company Incorporated, 1996.
[9] K.S. Kim, P. Tarakeshwar, J.Y. Lee, Chem. Rev. 100 (2000) 4145.
[10] L. Brunsveld, B. Folmer, E. Meijer, R. Sijbesma, Chem. Rev. 101 (2001) 4071.
[11] E. Arunan, H. Gutowsky, Lett. Editor 4295 (1993) 2.
[12] M.O. Sinnokrot, E.F. Valeev, C.D. Sherrill, J. Am. Chem. Soc. 124 (2002) 10887.
[13] S. Tsuzuki, K. Honda, T. Uchimaru, M. Mikami, K. Tanabe, J. Am. Chem. Soc. 124 (2002) 104.
[14] B.W. Hopkins, G.S. Tschumper, J. Phys. Chem. A 108 (2004) 2941.
[15] M.O. Sinnokrot, C.D. Sherrill, J. Phys. Chem. A 108 (2004) 10200.
[16] C. Chipot, R. Jaffe, B. Maigret, D.A. Pearlman, P.A. Kollman, J. Am. Chem. Soc. 118 (1996) 11217.
[17] T. Ebata, T. Watanabe, N. Mikami, J. Phys. Chem. 99 (1995) 5761.
[18] G. Pietraperzia et al., J. Phys. Chem. A 115 (2011) 9603.
[19] E.B. Erba, R. Zenobi, Annu. Rep. Prog. Chem., Sect. C: Phys. Chem. 107 (2011) 199.
[20] Y. Mercier, F. Santoro, M. Reguero, R. Improta, J. Phys. Chem. B 112 (2008) 10769.
[21] F. Santoro, V. Barone, A. Lami, R. Improta, Phys. Chem. Chem. Phys. 12 (2010) 4934.
[22] R. Improta, V. Barone, A. Lami, F. Santoro, J. Phys. Chem. B 113 (2009) 14491.
[23] K.E.P. Riley, Chem. Rev. 110 (2010) 5023.
[24] P. Hobza, Annu. Rep. Prog. Chem., Sect. C: Phys. Chem. 107 (2011) 148.
[25] P. Procacci, Annu. Rep. Prog. Chem., Sect. C: Phys. Chem. 107 (2011) 242.
[26] E.R. Johnson, R.A. Wolkow, G.A. DiLabio, Chem. Phys. Lett. 394 (2004) 334.
[27] C.D. Sherrill, Rev. Comput. Chem. (2009) 1.
[28] E.G. Hohenstein, S.T. Chill, C.D. Sherrill, J. Chem. Theory Comput. 4 (2008) 1996.
[29] G.A. DiLabio, Chem. Phys. Lett. 455 (2008) 348.
[30] S. Grimme, J. Antony, S. Ehrlich, H. Krieg, J. Chem. Phys. 132 (2010) 154104.
[31] J.D. Chai, M. Head-Gordon, Phys. Chem. Chem. Phys. 10 (2008) 6615.
[32] E.H.A. Beckers, P. Jonkheijm, A.P.H.J. Schenning, S.C.J. Meskers, R.A.J. Janssen, ChemPhysChem 6 (2005) 2029.
[33] Z. Chen, A. Lohr, C.R. Saha-Möller, F. Würthner, Chem. Soc. Rev. 38 (2008) 564.
[34] C. Zhang, Y.S. Zhao, J. Yao, New J. Chem. 35 (2011) 973.
[35] F. Steuber et al., Adv. Mater. 12 (2000) 130.
[36] F. Shen et al., J. Phys. Chem. A 112 (2008) 2206.
[37] Y. Li, S. Liu, M. Chen, F. Ma, J. Photochem. Photobiol., A 205 (2009) 139.
[38] M.J. Frisch, G.W. Trucks, H.B. Schlegel, et al., Gaussian Revision A02, Gaussian, Inc., Wallingford, CT, 2009.
[39] M. Cossi, V. Barone, R. Cammi, J. Tomasi, Chem. Phys. Lett. 255 (1996) 327.
[40] T. Lu, F. Chen, J. Comput. Chem. 33 (2012) 580.
[41] J. Locker, VMD Program Revision: 1.9, 2007.
[42] H.P.L.P. Flükiger, S. Portmann, J. Weber MOLEKEL 4.3.3, J. Swiss Center for Scientific Computing: Manno, Switzerland, 2002.
[43] S.K.E.R. Johnson, P. Mori-Sánchez, J. Contreras-García, J. Am. Chem. Soc. 132 (2010) 6498.